Regulation of CNS and motor axon guidance in *Drosophila* by the receptor tyrosine phosphatase DPTP52F

Benno Schindelholz[1],*, Matthias Knirr[1],‡, Rahul Warrior[2] and Kai Zinn[1],§

[1]Division of Biology, California Institute of Technology, Pasadena, CA 91125, USA
[2]Department of Biology, University of Southern California, 835 W 37th Street, Los Angeles, CA 90089, USA
*Present address: The Genetics Company, Winterthurstr. 190, 8057 Zürich, Switzerland
‡Present address: Friedrich-Miescher-Labor der Max-Planck-Gesellschaft, Spemannstr. 37, D-72070 Tübingen, Germany
§Author for correspondence (e-mail: zinnk@its.caltech.edu)

SUMMARY

Receptor-linked protein tyrosine phosphatases (RPTPs) regulate axon guidance and synaptogenesis in *Drosophila* embryos and larvae. We describe DPTP52F, the sixth RPTP to be discovered in *Drosophila*. Our genomic analysis indicates that there are likely to be no additional RPTPs encoded in the fly genome. Five of the six *Drosophila* RPTPs have *C. elegans* counterparts, and three of the six are also orthologous to human RPTP subfamilies. DPTP52F, however, has no clear orthologs in other organisms. The DPTP52F extracellular domain contains five fibronectin type III repeats and it has a single phosphatase domain. DPTP52F is selectively expressed in the CNS of late embryos, as are DPTP10D, DLAR, DPTP69D and DPTP99A. To define developmental roles of DPTP52F, we used RNA interference (RNAi)-induced phenotypes as a guide to identify *Ptp52F* alleles among a collection of EMS-induced lethal mutations. *Ptp52F* single mutant embryos have axon guidance phenotypes that affect CNS longitudinal tracts. This phenotype is suppressed in *Dlar Ptp52F* double mutants, indicating that DPTP52F and DLAR interact competitively in regulating CNS axon guidance decisions. *Ptp52F* single mutations also cause motor axon phenotypes that selectively affect the SNa nerve. DPTP52F, DPTP10D and DPTP69D have partially redundant roles in regulation of guidance decisions made by axons within the ISN and ISNb motor nerves.

Key words: Receptor tyrosine phosphatase, PTP, *Drosophila*, Neural development, Axon guidance, Neuromuscular system, Genomics, Motor axon, RNAi

INTRODUCTION

Receptor-linked protein tyrosine phosphatases (RPTPs) regulate axon guidance and synaptogenesis decisions in *Drosophila* embryos and larvae. Five *Drosophila* RPTPs have been described, and four of these are selectively expressed on central nervous system (CNS) axons (Desai et al., 1994; Hariharan et al., 1991; Streuli et al., 1989; Sun et al., 2000; Tian et al., 1991; Yang et al., 1991). They do not obviously define distinct sets of pathways, as they appear to be expressed on most or all CNS axons. DPTP4E mRNA is widely expressed, but its protein distribution pattern is unknown (Oon et al., 1993).

The four 'neural' RPTPs DPTP10D, DLAR, DPTP69D and DPTP99A have been studied using genetics. All four regulate axon guidance decisions in embryos (Desai et al., 1996; Desai et al., 1997; Krueger et al., 1996; Sun et al., 2000; Sun et al., 2001; Wills et al., 1999). *Ptp69D*, *Dlar* (*Lar* – FlyBase) and *Ptp10D* mutations also cause optic lobe innervation defects in larvae and pupae (Garrity et al., 1999; Newsome et al., 2000) (T. Suzuki et al., and Q. Sun and K. Z., unpublished).

Single mutants that lack DLAR or DPTP69D have guidance phenotypes affecting specific pathway decisions made by embryonic motor axons (Desai et al., 1996; Krueger et al., 1996). However, most guidance decisions within the neuromuscular system are altered only when specific combinations of two or more RPTPs are eliminated, indicating that RPTPs can have partially redundant functions at growth cone choice points (Desai et al., 1996; Desai et al., 1997; Sun et al., 2000; Sun et al., 2001).

RPTPs can also have 'competitive' activities, in a formal genetic sense. DLAR and DPTP99A function in opposition to each other in regulating entry of the ISNb motor nerve into its target ventrolateral muscle (VLM) field (Desai et al., 1997). The Abl tyrosine kinase and its substrate Ena are also involved in DLAR signaling at this decision point (Wills et al., 1999).

Little is known about the biochemical mechanisms involved in control of motor axon guidance by RPTPs. The ligands and/or co-receptors that might interact with their extracellular (XC) domains have not been identified. The *in vivo* substrates for fly RPTPs are also unknown, although several proteins that they can dephosphorylate in vitro or in transfected cells have been described (Fashena and Zinn, 1997; Wills et al., 1999).

None of the previously characterized Rptp single mutants has strong phenotypes that affect the array of axons within the CNS, as assayed by staining with several different antibody

markers. Removal of both DPTP10D and DPTP69D, however, generates a unique phenotype in which many longitudinal axons abnormally cross the midline (Sun et al., 2000). The *Ptp10D Ptp69D* double mutation interacts with *roundabout*, *commissureless* and *slit*, a set of mutations defining a pathway that repels longitudinal axons from the midline and prevents commissural axons from recrossing it (Zinn and Sun, 1999).

We describe DPTP52F, which is probably the last remaining RPTP encoded in the *Drosophila* genome. *Ptp52F* mutations cause specific CNS and motor axon guidance phenotypes, and exhibit genetic interactions with mutations in the other Rptp genes.

MATERIALS AND METHODS

Genetics

In an screen to isolate mutations in the *Drosophila Lissencephaly 1* (*DLis-1*; *Lis1* – FlyBase) gene, 18,000 independent EMS mutations were isolated (J. Duncan and R. W.; a complete description will be published elsewhere). 183 mutations were identified that are lethal when placed in *trans* to the deficiency *Df(2R)JP6*, which includes the *DLis-1* and *Ptp52F* genes. These mutations were subdivided by testing for lethality over two overlapping deficiencies, *Df(2R)JP4* and *Df(2R)JP8* (Fig. 1). 70 mutations in 13 complementation groups were lethal in *trans* to all three deficiencies, and eight *Ptp52F* alleles were identified among these.

For genetic interaction studies, we used the alleles *Ptp10D[1]* (Sun et al., 2000), *Dlar[5.5]* (Krueger et al., 1996), the transheterozygous combination *Ptp69D[1]/Df(3L)8ex25* (Desai et al., 1996) and *Ptp99A[1]* (Hamilton et al., 1995).

Molecular biology

PCR amplification of DPTP52F, DPTP26C and DPTP36E fragments was performed on phage stocks of a 9-12 hr λgt11 library (Zinn et al., 1988) using primers designed from genomic sequences. cDNA clones were isolated from this and other libraries, including a random-primed 9-12 hour λZAPII library (K. Z., unpublished), by hybridization to these PCR fragments. We were only able to obtain one cDNA clone encoding a portion of the DPTP52F extracellular (XC) domain. The sequence of this cDNA could encode an open reading frame of 881 amino acids, corresponding to the C-terminal section of the predicted protein CG18243 (1419 amino acids) in Release 2 of GadFly. A number of in-frame stop codons are located upstream of the ATG for the reading frame, which is at nucleotide 580 of our cDNA. However, a comparison of the sequence of our cDNA to the genome sequence revealed that an intron upstream of this ATG had not been completely removed. In the cDNA, the 5′ splice site of this intron is fused to sequences within the intron, and the fusion joins the 5′ splice site to a site near the branchpoint, 14 nucleotides 5′ to the acceptor site. This cDNA is thus a copy of an aberrantly spliced RNA. All other introns within the cDNA sequence were removed in a normal manner. To define the complete coding region for DPTP52F, we then performed reverse transcription-PCR (RT-PCR) experiments on primary embryonic first-strand cDNA preparations. We used a 3′ primer within the cDNA, downstream of the aberrantly spliced intron, and a series of 5′ primers, the most 5′ of which was upstream of the ATG of CG18243 (in the presumed 5′ UTR of the CG18243 mRNA; primer sequences available on request). (CG18243 has no ESTs, so its predicted mRNA has no 5′ UTR; it begins with the ATG of the predicted protein.) Analysis of the cloned PCR products revealed that the DPTP52F protein sequence begins with the initiating methionine of CG18243. There are several in-frame stop codons immediately upstream of this ATG, so the protein must start here. The authentic DPTP52F sequence is very similar to CG18243, except that the intron

that was incompletely removed from our cDNA (intron 3) does not use the predicted CG18243 5′ splice site, but rather uses a 5′ splice site 42 nucleotides downstream. This is the same 5′ splice site that was fused to the branchpoint sequence in our clone. The actual 3′ splice site of this intron is as predicted for CG18243. Joining these splice sites preserves the CG18243 reading frame, so the DPTP52F protein contains an extra 14 amino acids, making the entire preprotein 1433 amino acids in length.

dsRNA-mediated genetic interference

This was performed essentially as described in the Carthew laboratory protocol (http://www.pitt.edu/~carthew/manual/RNAi_Protocol.html) (Kennerdell and Carthew, 1998; Schmid et al., 2001). Sequences to be transcribed into dsRNAs were cloned into Bluescript KS+, linearized with the appropriate restriction enzymes, and transcribed in vitro with Ambion T3 and T7 Megascript kits following the manufacturer's instructions. Transcripts were annealed in injection buffer (0.1 mM NaPO4, pH 7.8/5 mM KCl) after heating to 95°C for 1 minute and cooled gradually to room temperature by placing the water bath in a foam box over a 18 hour period. We typically injected ~0.1 nl of 0.5-2.0 μM solutions of dsRNAs. The *Ptp52F* dsRNAs corresponded to *Ptp52F* sequences spanning nucleotides 1279-2444 and nucleotides 2105-3998 (counting from the initiating ATG). Cages were set up using 2- to 4-day-old Oregon R flies. Eggs were collected over a 15- to 30-minute period on grape juice agar plates for subsequent injection. The eggs were lined up lengthwise on double stick tape on a glass slide and immersed in halocarbon oil. Syncitial blastoderm embryos were injected at ~50% egg length (EL) using an Eppendorf transjector. After injection, embryos were allowed to develop to stage 16-17 under oil in a moist chamber.

Antibody production

A fragment of the extracellular domain of DPTP52F (amino acids 572-1037) tagged with His_6 was expressed in *E. coli* at the Caltech Protein Expression Facility. Monoclonal antibodies (mAbs) against this fusion protein were generated at the Caltech Monoclonal Antibody Facility and screened based on their ability to recognize the fusion protein on dot blots and by staining of whole mount embryos. mAb 13B8, which worked well for immunostaining of whole mount embryos (Fig. 2), was used at a 1:3 dilution.

Immunohistochemistry

Embryos were collected from crosses between flies bearing various combinations of mutant alleles. The desired mutant embryos were identified based on the absence of staining with mAbs specific for each RPTP and/or by the absence of staining with anti-β-galactosidase mAb (Promega), which detects the presence of the *lacZ* gene on the balancer chromosomes. Anti-RPTP mAbs used were 3A6 (DPTP99A) (Tian et al., 1991), 45E10 (DPTP10D) (Tian et al., 1991), 3F11 (DPTP69D) (Desai et al., 1994) and 8C4 (DLAR) (Sun et al., 2000). Mutant embryos were then restained with mAb 1D4 (Van Vactor et al., 1993) to reveal motor axon and CNS pathways, dissected, and photographed with a Magnafire digital camera on a Zeiss Axioplan microscope using Nomarski optics. All mAb supernatants were used at 1:5 to 1:10 dilutions. Antibody staining using horseradish peroxidase (HRP) immunohistochemistry was performed as described (Patel, 1994). Amplification of the HRP signal was performed using a Vectastain Elite kit (Vector Laboratories).

Database searches

Celera scaffold sequence (Venter et al., 2001) was searched with blastn using cDNA sequences encoding each human PTP named in a publication. PTP protein sequences were used to search the same database using tblastn, and correlations were made between scaffolds and known RPTPs. Unknown PTP-related sequences were examined further to determine if they are pseudogenes. The names of all 19 human RPTP-like proteins, with an Accession Number for
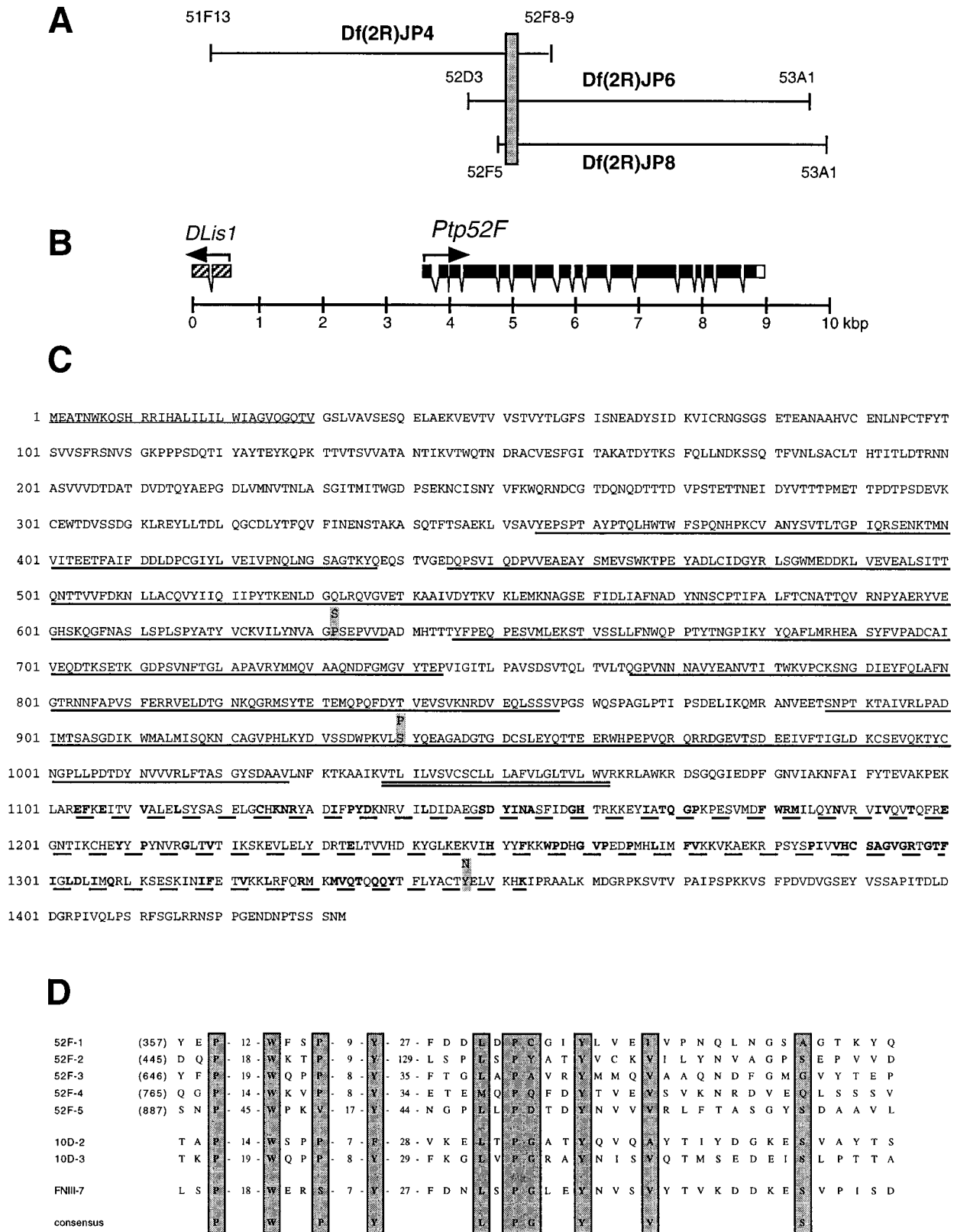
A

51F13   Df(2R)JP4   52F8-9

52D3   Df(2R)JP6   53A1

52F5   Df(2R)JP8   53A1

B

DLis1   Ptp52F

0   1   2   3   4   5   6   7   8   9   10 kbp

C

```
   1 MEATNWKQSH RRIHALILIL WIAGVQGQTV GSLVAVSESQ ELAEKVEVTV VSTVYTLGFS ISNEADYSID KVICRNGSGS ETEANAAHVC ENLNPCTFYT

 101 SVVSFRSNVS GKPPPSDQTI YAYTEYKQPK TTVTSVVATA NTIKVTWQTN DRACVESFGI TAKATDYTKS FQLLNDKSSQ TFVNLSACLT HTITLDTRNN

 201 ASVVVDTDAT DVDTQYAEPG DLVMNVTNLA SGITMITWGD PSEKNCISNY VFKWQRNDCG TDQNQDTTTD VPSTETTNEI DYVTTTPMET TPDTPSDEVK

 301 CEWTDVSSDG KLREYLLTDL QGCDLYTFQV FINENSTAKA SQTFTSAEKL VSAVYEPSPT AYPTQLHWTW FSPQNHPKCV ANYSVTLTGP IQRSENKTMN

 401 VITEETFAIF DDLDPCGIYL VEIVPNQLNG SAGTKYQEQS TVGEDQPSVI QDPVVEAEAY SMEVSWKTPE YADLCIDGYR LSGWMEDDKL VEVEALSITT

 501 QNTTVVFDKN LLACQVYIIQ IIPYTKENLD GQLRQVGVET KAAIVDYTKV KLEMKNAGSE FIDLIAFNAD YNNSCPTIFA LFTCNATTQV RNPYAERYVE

 601 GHSKQGFNAS LSPLSPYATY VCKVILYNVA GPSEPVVDAD MHTTTYFPEQ PESVMLEKST VSSLLFNWQP PTYTNGPIKY YQAFLMRHEA SYFVPADCAI

 701 VEQDTKSETK GDPSVNFTGL APAVRYMMQV AAQNDFGMGV YTEPVIGITL PAVSDSVTQL TVLTQGPVNN NAVYEANVTI TWKVPCKSNG DIEYFQLAFN

 801 GTRNNFAPVS FERRVELDTG NKQGRMSYTE TEMQPQFDYT VEVSVKNRDV EQLSSSVPGS WQSPAGLPTI PSDELIKQMR ANVEETSNPT KTAIVRLPAD

 901 IMTSASGDIK WMALMISQKN CAGVPHLKYD VSSDWPKVLS YQEAGADGTG DCSLEYQTTE ERWHPEPVQR QRRDGEVTSD EEIVFTIGLD KCSEVQKTYC

1001 NGPLLPDTDY NVVVRLFTAS GYSDAAVLNF KTKAAIKVTL ILVSVCSCLL LAFVLGLTVL WVRKRLAWKR DSGQGIEDPF GNVIAKNFAI FYTEVAKPEK

1101 LAREFKEITV VALELSYSAS ELGCHKNRYA DIFPYDKNRV ILDIDAEGSD YINASFIDGH TRKKEYIATQ GPKPESVMDF WRMILQYNVR VIVQVTQFRE

1201 GNTIKCHEYY PYNVRGLTVT IKSKEVLELY DRTELTVVHD KYGLKEKVIH YYFKKWPDHG VPEDPMHLIM FVKKVKAEKR PSYSPIVVHC SAGVGRTGTF

1301 IGLDLIMQRL KSESKINIFE TVKKLRFQRM KMVQTQQQYT FLYACTYELV KHKIPRAALK MDGRPKSVTV PAIPSPKKVS FPDVDVGSEY VSSAPITDLD

1401 DGRPIVQLPS RFSGLRRNSP PGENDNPTSS SNM
```

D

52F-1	(357) Y E	P	12	W F S	P	9	V	27	F D D	L D F C	G I	Y L	V E V P N Q L N G S A G T K Y Q
52F-2	(445) D Q	P	18	W K T	P	9	V	129	L S P	L S P Y	A T	Y V C K	V I L Y N V A G P S E P V V D
52F-3	(646) Y F	P	19	W Q P	P	8	V	35	F T G	L A P A V	R	Y M M Q	V A A Q N D F G M G V Y T E P
52F-4	(765) Q G	P	14	W K V	P	8	V	34	E T E	M Q P Q F	D	Y T V E	V S V K N R D V E Q L S S S V
52F-5	(887) S N	P	45	W P K	V	17	V	44	N G P	L L F D T	D	Y N V V	V R L F T A S G Y S D A A V L
10D-2	T A	P	14	W S P	P	7	P	28	V K E	L T P G	A T	Y Q V Q A	Y T I Y D G K E S V A Y T S
10D-3	T K	P	19	W Q P	P	8	V	29	F K G	L V F G	R A	Y N I S	V Q T M S E D E I S L P T T A
FNIII-7	L S	P	18	W E R	S	7	V	27	F D N	L S P G	L E	Y N V S	V Y T V K D D K E S V P I S D
consensus		P		W			Y			L P G		Y	V S

Fig. 1. The *Ptp52F* gene. (A) Map of the deficiencies used for the EMS lethal screen. The position of the *Ptp52F* gene is indicated by the shaded bar. (B) Exon maps of *Ptp52F* and the adjacent *DLis1* genes; distal (toward the telomere) is towards the left, so the orientation is flipped relative to A. (C) Sequence of the DPTP52F preprotein. Indicated sequences are: putative signal sequence, thin underline; FN3 repeats, thick underlines; putative transmembrane domain, double underline; PTP domain, broken underline; bold, highly conserved PTP domain residues; letters in shaded bars, amino acid changes produced by mutations. (D) Lineup of the DPTP52F FN3 repeats with two FN3 repeats from DPTP10D and the seventh FN3 repeat in human fibronectin. Shaded bars, conserved residues. Consensus residues indicated in bold.

Fig. 2. Expression of DPTP52F protein. Whole-mount embryos were stained with mAb 13B8 using HRP immunohistochemistry. (A) A ventral view of a gastrulating embryo, showing DPTP52F at the edges of the ventral furrow (arrow). At this stage, DPTP52F is on the membranes of all cells in the embryo at lower levels. (B) A side view (anterior towards the left) of a stage 15 embryo. The ventral nerve cord (arrow) expresses DPTP52F. (C) Two segments of a dissected CNS from a stage 15 wild-type embryo. DPTP52F is expressed on cell bodies; axon tracts (arrow) are lighter. (D) A dissected CNS from a stage 15 $Ptp52F^{18.3}$ embryo. No staining is observed.
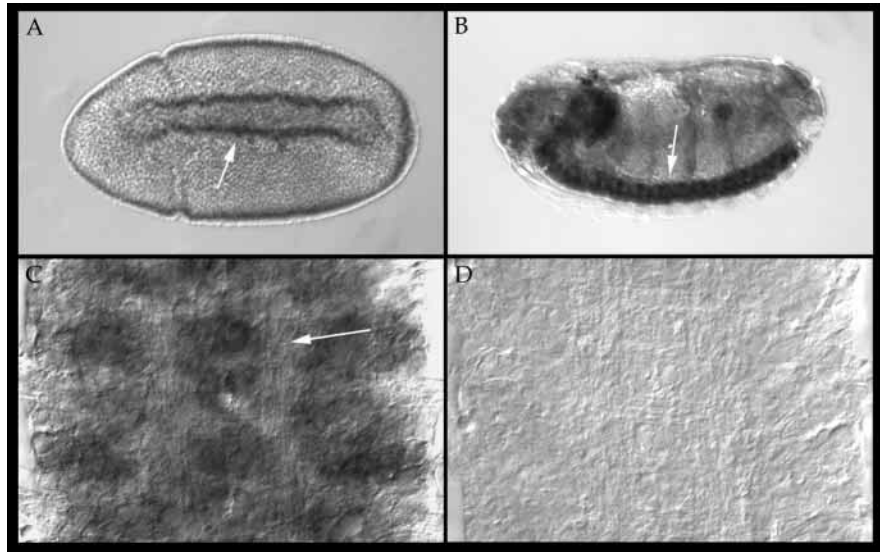
a reference sequence for each, are HPTPβ=PTPβ (X54131), HPTPη=DEP-1=CD148 (D37781), GLEPP-1=PTP-U2 (U20489), Sap-1 (D15049), PTP-RQ=PTP-GMC1 (human fragment (134 amino acids) is AF169351, rat rPTP-GMC1 (full sequence) is AF063249), LAR (Y00815), PTPδ (L38929), PTPσ (U35234), PTPμ (X58288), PTPκ (L77886), RPTPρ=PTPRT (AF043644), PTPo=PTPRO=hPTP-J=PCP-2=R-PTP-ψ=PTP-π,=PTPRU=PTPρ (U71075), PTPζ=RPTPβ (M93426), PTPγ (L09247), PTPα (M34668), PTPε (X54134), CD45=LCA (Y00062), IA-2=512 antigen=PTP35 (L18983), and phogrin=IA-2β=PTP-NP=PTP-IAR=ICAAR=PTP-X (AB002385) (the last two are catalytically inactive). The reference sequences and scaffolds of the 16 cytoplasmic PTPs and the nine new PTP pseudogenes we defined are available on request. Our conclusions regarding orthologous relationships between fly, worm and human RPTPs differ from those in a recent review (Walchli et al., 2000). These authors defined orthologs based solely on E values of blastp searches with PTP domains, and did not consider whether homology extends over the entire protein. As these E values are very similar for many pairs of PTP domains, and such values are highly sensitive to gap length, this is not a good way to determine orthologs. For example, they assigned DPTP69D as the CD45 ortholog, and DPTP99A as the PTPγ ortholog, but there are no relationships between the XC domain sequences within these pairs.

RESULTS

Identification and characterization of the sixth *Drosophila* RPTP gene

The five previously known *Drosophila* RPTP genes were all identified by low-stringency hybridization and PCR experiments (Hariharan et al., 1991; Streuli et al., 1989; Tian et al., 1991; Yang et al., 1991; Oon et al., 1993). Three cytoplasmic PTP genes have also been characterized: *csw*, *Ptp-ER* and *Ptp61F* (Karim and Rubin, 1999; McLaughlin and Dixon, 1993; Perkins et al., 1992). Mutant alleles have been isolated for all of the *Rptp* and cytoplasmic PTP genes except *Ptp4E* and *Ptp61F*.

We performed searches of the Berkeley *Drosophila* Genome Project (BDGP) genomic sequence database for additional PTP sequences in 1998 and 1999. When these searches were conducted, about 25% of the sequence was available, but much

of it was in unordered pieces. We found PTP sequence fragments at three cytological locations: 26C, 36E and 52F. These fragments all encoded a sequence closely related to VHCSAGRGV, the canonical PTP active-site motif (Fauman and Saper, 1996). We isolated and sequenced cDNA clones encoding these three PTPs. Analysis of these sequences showed that we had identified two cytoplasmic PTPs (DPTP26C and DPTP36E) and an RPTP (DPTP52F).

Our analysis of cDNA clones and PCR products showed that the DPTP52F preprotein is 1433 amino acids in length (see Materials and Methods for details). The amino acid sequence immediately following the initiating methionine has a 23 amino acid uncharged region (amino acids 15-38) and resembles a signal peptide. A single predicted transmembrane domain is located at residues 1038-1062. The XC domain has 17 potential N-linked glycosylation sites. Its C-terminal region (amino acids ~370-1037) contains five fibronectin type III (FN3) repeats like those found in other *Drosophila* RPTPs. FN3 repeats are also found in many adhesion and extracellular matrix molecules (Fig. 1D). The N-terminal 370 amino acids of the XC domain is not significantly related to any other sequences in the database.

Among published RPTP sequences, DPTP52F is most similar overall to DPTP4E (42% similarity), although they differ in the number of FN3 repeats in their XC domains (five versus 13). DPTP52F has a single cytoplasmic phosphatase domain that is 32-36% identical in sequence to the PTP domains of the other known *Drosophila* RPTPs.

We were unable to detect DPTP52F mRNA by in situ hybridization to embryos, suggesting that it is expressed at very low levels. We generated mAbs against the XC domain of DPTP52F, and used these to perform immunohistochemical staining of whole-mount embryos. Expression of DPTP52F is observed at the cellular blastoderm stage. During formation of the ventral furrow, DPTP52F can be detected on cells flanking the invaginating region (Fig. 2A).

Later in development (stages 13-17), DPTP52F is selectively expressed in the CNS (Fig. 2B). This CNS specificity resembles that seen for the four 'neural RPTPs' DPTP10D, DLAR, DPTP69D and DPTP99A (Desai et al., 1994; Hariharan et al., 1991; Sun et al., 2000; Tian et al., 1991; Yang
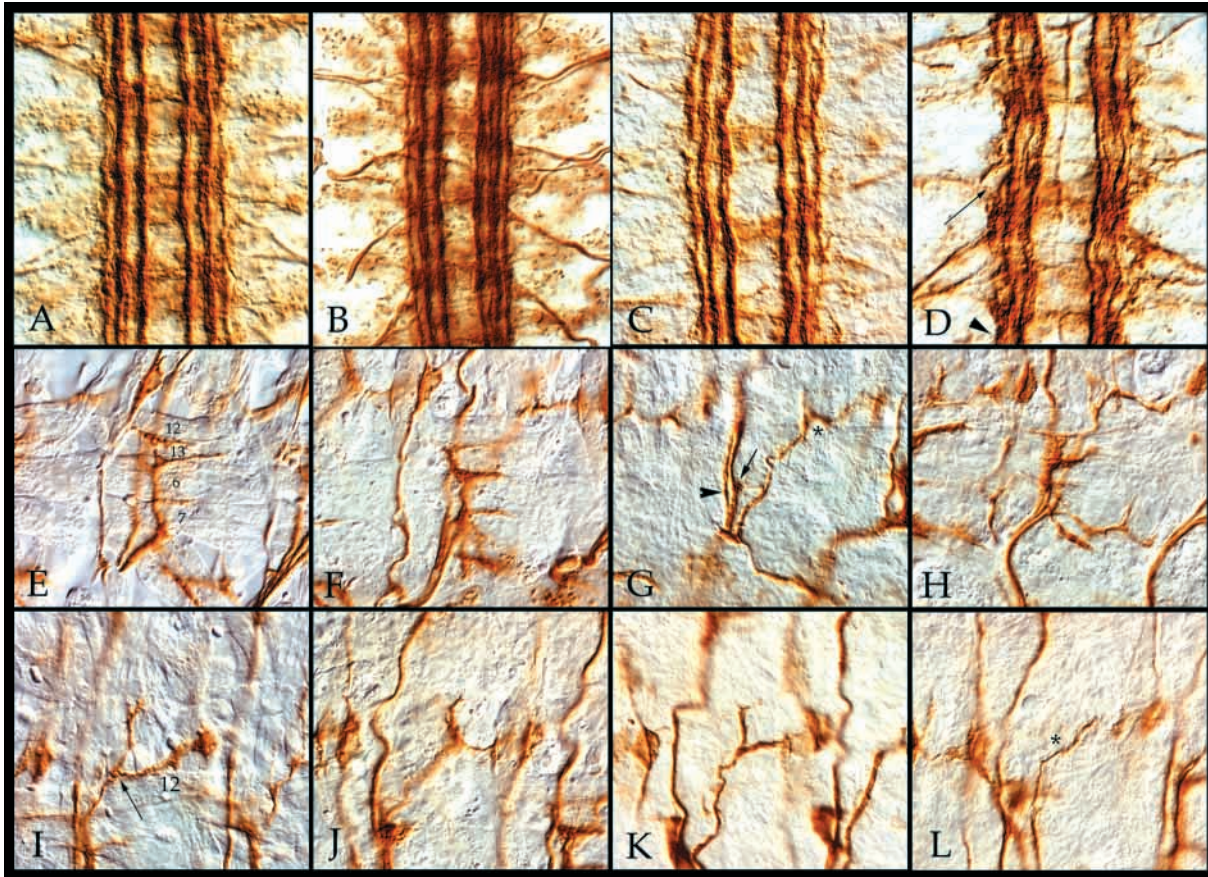
Fig. 3. CNS and motor axon phenotypes produced by RNAi. Dissected late stage 16 embryos stained with mAb 1D4. Column 1 (A,E,I), wild-type. Column 2 (B,F,J), embryos injected with injection buffer. Column 3 (C,G,K), embryos injected with *Dlar* dsRNA. Column 4 (D,H,L), embryos injected with *Ptp52F* dsRNA. Row 1 (A-D), the CNS (anterior up); note the 3 straight longitudinal bundles on each side of the midline in A-C. Arrow in D indicates a break in the outer 1D4 bundle; arrowhead indicates abnormal fasciculation of the middle and outer bundles. Row 2 (E-H), ISNb (anterior towards the left); note the 3 characteristic synaptic branches in E,F,H; muscles are numbered in E. Arrow in G, bypass ISNb; arrowhead, ISN; asterisk, SNa. Row 3 (I-L), SNa; note the characteristic bifurcation in I-K, indicated by arrow in (I); muscle 12 is also labeled. Asterisk in L, approximate position of missing bifurcation.

et al., 1991). These RPTPs, however, are localized to axons and are present only at very low levels on neuronal cell bodies. By contrast, DPTP52F appears to be expressed primarily on neuronal cell bodies (Fig. 2C).

By amplifying the antibody signal, we can sometimes detect CNS axon bundles that appear to be positive for DPTP52F staining (data not shown). We cannot state with certainty that these axons express DPTP52F, however, as they are on top of positive cell bodies, and some or all of the brown color of the axon bundles could be due to these underlying cells.

The absence of motor axon staining with anti-DPTP52F is not surprising, because these axon bundles are thin and therefore do not stain strongly. We also cannot visualize expression of DLAR or DPTP99A on motor axons in wild-type embryos, and DPTP10D can only be detected on the SNa nerve (Sun et al., 2000; Sun et al., 2001). Determining that these other RPTPs are axonally localized was not a problem, however, because visualization of positive axon bundles within the CNS was not impaired by staining of underlying cell bodies.

Df(2R)JP4/Df(2R)JP8 embryos, which have a complete deletion of the *Ptp52F* gene (Fig. 1A), do not stain with anti-

DPTP52F mAbs. Embryos homozygous for point mutations in *Ptp52F* (see below) also do not stain (Fig. 2D). These results show that the mAbs selectively recognize DPTP52F.

Perturbation of DPTP52F expression using RNAi produces axon guidance phenotypes

Injected double-stranded RNA (dsRNA) is a potent and specific inhibitor of gene expression in *Drosophila*; this method of gene expression blockage is called RNA interference (RNAi) (Kennerdell and Carthew, 1998; Misquitta and Paterson, 1999); see also (Schmid et al., 2001). We initially used RNAi to evaluate the functions of DPTP52F during embryonic development. We examined motor axon and CNS phenotypes in these embryos by staining them with mAb 1D4 (Van Vactor et al., 1993), which recognizes motor axons in the periphery and three paired longitudinal bundles within the CNS. In abdominal segments A2-A7, ~32 motor axons exit the CNS within the ISN (intersegmental nerve) and SN (segmental nerve) roots; these then split into five pathways that innervate 30 muscle fibers (Keshishian et al., 1996). The SNa and SNc pathways emerge from the SN root, and the ISN, ISNb, and ISNd pathways arise

from the ISN root. ISNb and ISNd are also known as SNb and SNd.

To evaluate the efficacy of RNAi for perturbation of *Rptp* gene expression, we first injected *Dlar* dsRNA into embryos and allowed them to develop to stage 16-17. Injection of buffer produced no phenotypes (Fig. 3B,F,J), whereas injection of *Dlar* dsRNA phenocopied the characteristic *Dlar* mutant ISNb phenotype, known as parallel bypass (Fig. 3G). In parallel bypass hemisegments, ISNb leaves the ISN tract in an apparently normal manner and continues to extend dorsally, but fails to innervate its VLM targets (Krueger et al., 1996). In *Dlar* RNAi embryos, 15% of hemisegments had parallel bypass phenotypes. This penetrance is very similar to that observed for zygotic *Dlar* null mutants (18%) (Desai et al., 1997). SNa and CNS pathways are not affected in *Dlar* mutants (Krueger et al., 1996), and these also appeared normal in *Dlar* dsRNA-injected embryos (Fig. 3C,K).

We then injected two different *Ptp52F* dsRNAs derived from overlapping sections of the *Ptp52F* cDNA. The two dsRNAs produced identical phenotypes in which the 1D4-positive bundles in the CNS are irregular and abnormally fasciculated. The outer 1D4-positive bundle is often missing (Fig. 3D).

The ISNb, ISNd and SNc motor nerves appeared identical to wild type in *Ptp52F* RNAi embryos (Fig. 3H; data not shown). The SNa nerve, however, displayed a clear and diagnostic phenotype. SNa has a characteristic bifurcated morphology. The bifurcation occurs at a choice point located between muscles 22 and 23. The posterior (or lateral) branch of the SNa innervates muscles 5 and 8, and the anterior (or dorsal) branch innervates muscles 21-24 (Fig. 3I). In embryos injected with *Ptp52F* dsRNA, either the posterior or anterior branch was sometimes missing (Fig. 3L). The penetrance of this bifurcation phenotype was 18%. In summary, our RNAi experiments suggested that DPTP52F is involved in guidance of longitudinal axons within the CNS and in bifurcation of the SNa motor nerve.

Identification of *Ptp52F* mutants

We examined a collection of EMS-induced mutations that are lethal over *Df(2R)JP4*, *Df(2R)JP6* and *Df(2R)JP8* (Fig. 1A) for the *Ptp52F* CNS and SNa phenotypes that we had defined using RNAi. There are 13 lethal complementation groups in this interval. We collected embryos from lines representing each of these complementation groups and stained them with mAb 1D4. Mutations within one complementation group produced phenotypes identical to those we had observed with RNAi. This group consists of eight alleles. We sequenced the *Ptp52F* gene from three of these alleles, and found the following mis-sense mutations (Fig. 1C): *Ptp52F[18.3]*, Ser to Pro in the fifth FN3 repeat (S941P), *Ptp52F[7.8.1]*, Pro to Ser in the second FN3 repeat (P633S), and *Ptp52F[8.10.3]*, Tyr to Asn in the PTP domain (Y1348N).

Transheterozygous *Ptp52F[18.3]/Df(2R)JP4* flies can survive until the first instar larval phase. *Ptp52F* embryos appear morphologically normal during all phases of development. The peripheral nervous system (PNS) displays no defects, and the pattern of body wall muscle fibers is also normal. There are also no abnormalities in the patterns of expression of the Even-skipped (Eve) and Engrailed (En) homeodomain proteins during segmentation or later within the CNS, suggesting that the fates of Eve- and En-expressing cells are not altered by these mutations (data not shown).

Table 1. SNa phenotypes in *Rptp* mutant embryos

Genotype	n	t	M	S	A	–
			Phenotype (%)*			
Ptp52F						
Ptp52F[18.3]	145	37	19	5	14	0
Ptp52F[18.3]/Df(2R)JP4	137	41	20	7	10	4
Ptp52F[18.3]/Df(2R)JP8	149	32	9	3	19	0
Ptp52F[8.10.3]	150	28	9	0	18	0
Ptp52F[8.10.3]/Df(2R)JP4	100	36	12	4	20	0
Ptp52F[8.10.3]/Df(2R)JP8	109	22	7	0	16	0
Ptp52F[7.8.1]	138	27	14	0	27	0
Ptp52F[7.8.1]/Df(2R)JP4	101	36	12	2	22	0
Ptp52F[7.8.1]/Df(2R)JP8	129	22	7	0	16	0
Ptp10D Ptp52F						
Ptp10D[1]Ptp52F[18.3]	175	61	25	33	2	3
Ptp10D[1]Ptp52F[8.10.3]	100	45	17	23	5	0
Dlar Ptp52F						
Dlar[5.5]Ptp52F[18.3]	150	51	22	25	5	0
Ptp52F Ptp69D						
Ptp52F[18.3] Ptp69D[1]/Df(3L)8ex25	155	68	36	27	1	4
Ptp52F[8.10.3] Ptp69D[1]/Df(3L)8ex25	101	51	29	17	2	3
Ptp52F Ptp99A						
Ptp52F[18.3] Ptp99A[1]	145	33	25	3	2	2

n, number of hemisegments (A2-A7) scored.

a, additional branches at random positions; M, either posterior or anterior SNa branch is missing; S, SNa stalls near the bifurcation point; t, all affected SNa branches; –, the whole SNa branch is missing.

The numbers listed are % of hemisegments displaying a particular phenotype. Single *Dlar*, *Ptp10D*, *Ptp69D* and *Ptp99A* mutants are not listed, as these seldom display SNa phenotypes (<5% abnormal hemisegments).

Embryos homozygous for any of the three *Ptp52F* alleles express no detectable DPTP52F protein, as assayed by staining with anti-DPTP52F mAbs (Fig. 2D). Embryos homozygous for *Ptp52F[18.3]* or transheterozygous for *Ptp52F[18.3]* over *Df(2R)JP4* have approximately the same phenotypic penetrances. Thus, *Ptp52F[18.3]* may be a null allele. *Ptp52F[7.8.1]* or *Ptp52F[8.10.3]* produce the same phenotypes as *Ptp52F[18.3]*, but with somewhat lower penetrances, suggesting that they may be hypomorphic alleles (see Table 1, Table 2, Table 3). All of these data indicate that the phenotypes described in more detail below are due to the absence of the DPTP52F protein.

Ptp52F mutations perturb guidance of longitudinal pioneer axons

At stages 16 and 17, mAb 1D4 stains three distinct axon bundles in each longitudinal connective of the CNS, but does not stain any commissural bundles. In *Ptp52F[18.3]* and *Ptp52F[18.3]/Df(2R)JP4* embryos, a phenotype identical to that observed in *Ptp52F* dsRNA-injected embryos is observed, in which the longitudinal 1D4-positive bundles are wavy and irregular and the outer bundle is discontinuous or missing (Fig. 4B,C). The other two alleles produce weaker but similar CNS phenotypes (data not shown). We do not observe clear phenotypes in *Ptp52F* embryos stained with mAb BP102, which stains all CNS axons (Seeger et al., 1993). This suggests that only a subset of longitudinal axons is affected by the mutations.

To examine the establishment of longitudinal pathways, we analyzed earlier (stage 12 and 13) embryos. During stage 12, mAb 1D4 selectively stains the longitudinal pioneer neurons

Table 2. ISNb phenotypes in *Rptp* mutant embryos

		Phenotype (%)*		
Genotype	*n*	t	B	S
Ptp52F				
$Ptp52F^{18.3}$	145	7	1	6
$Ptp52F^{18.3}/Df(2R)JP4$	136	13	2	11
$Ptp52F^{18.3}/Df(2R)JP8$	150	5	1	4
$Ptp52F^{8.10.3}$	150	1	0	1
$Ptp52F^{8.10.3}/Df(2R)JP4$	100	4	0	4
$Ptp52F^{8.10.3}/Df(2R)JP8$	110	1	0	1
$Ptp52F^{7.8.1}$	138	3	0	3
$Ptp52F^{7.8.1}/Df(2R)JP4$	100	5	0	5
$Ptp52F^{7.8.1}/Df(2R)JP8$	130	2	0	2
Ptp10D Ptp52F				
$Ptp10D^{1}Ptp52F^{18.3}$	175	40	1	39
$Ptp10D^{1}Ptp52F^{8.10.3}$	100	32	2	30
Dlar and *Dlar Ptp52F*				
$Dlar^{5.5}/Dlar^{13.2}$	260	35	31	4
$Dlar^{5.5}Ptp52F^{18.3}$	146	40	23	17
Ptp69D and *Ptp52F Ptp69D*				
$Ptp69D^{1}/Df(3L)8ex25$	141	3	2	1
$Ptp52F^{18.3}Ptp69D^{1}/Df(3L)8ex25$	155	29	3	26
$Ptp52F^{8.10.3}Ptp69D^{1}/Df(3L)8ex25$	101	22	2	20
Ptp52F Ptp99A				
$Ptp52F^{18.3}Ptp99A^{1}$	145	15	1	14

n, number of hemisegments (A2-A7) scored.

B, bypass ISNbs; S, ISNbs that stall within the VLM field; t, all affected ISNb branches.

The numbers listed are % of hemisegments displaying a particular phenotype. Single *Ptp10D* and *Ptp99A* mutants are not listed, as these have no ISNb phenotypes (<2% abnormal hemisegments).

Table 3. ISN phenotypes in *Rptp* mutant embryos

		Phenotype (%)*				
Genotype	*n*	t	T	SB	FB	1–
Ptp52F						
$Ptp52F^{18.3}$	166	16	1	12	2	0
$Ptp52F^{18.3}/Df(2R)JP4$	157	20	0	17	3	0
$Ptp52F^{18.3}/Df(2R)JP8$	175	11	7	2	2	0
$Ptp52F^{8.10.3}$	177	5	0	5	0	0
$Ptp52F^{8.10.3}/Df(2R)JP4$	120	14	10	4	0	0
$Ptp52F^{8.10.3}/Df(2R)JP8$	127	4	4	0	0	0
$Ptp52F^{7.8.1}$	160	7	6	1	0	0
$Ptp52F^{7.8.1}/Df(2R)JP4$	117	15	6	9	0	0
$Ptp52F^{7.8.1}/Df(2R)JP8$	151	5	5	1	0	0
Ptp10D Ptp52F						
$Ptp10D^{1}Ptp52F^{18.3}$	207	67	40	23	4	0
$Ptp10D^{1}Ptp52F^{8.10.3}$	119	49	35	13	1	0
Dlar and *Ptp52F*						
$Dlar^{5.5}/Dlar^{13.2}$	256	41	22	19	0	0
$Dlar^{5.5}Ptp52F^{18.3}$	166	64	51	10	2	2
Ptp69D and *Ptp52F Ptp69D*						
$Ptp69D^{1}/Df(3L)8ex25$	131	1	1	0	0	0
$Ptp52F^{18.3}Ptp69D^{1}/Df(3L)8ex25$	182	58	1	57	1	0
$Ptp52F^{8.10.3}Ptp69D^{1}/Df(3L)8ex25$	117	47	7	40	0	0
Ptp52F Ptp99A						
$Ptp52F^{18.3}Ptp99A^{1}$	173	27	4	18	3	1

n, number of hemisegments (A2-A7) scored.

FB, ISNs that terminate at the first branchpoint; SB, ISNs that terminate at the second branchpoint; t, all affected ISN branches; T, ISNs that appear to reach the terminal arbor position, but are thin or bifurcated; 1–, ISNs that terminate proximal to the first branchpoint.

The numbers listed are % of hemisegments displaying a particular phenotype. Single *Ptp10D* and *Ptp99A* mutants are not listed, as these have no ISNb phenotypes (<2% abnormal hemisegments).

MP1, dMP2 and pCC. pCC pioneers the pCC/vMP2 pathway, which extends anteriorly over a 1D4-positive longitudinal glial cell, LG5 (Fig. 5A) (Seeger et al., 1993). When we examined *Ptp52F* mutants at slightly later stages (so as to be sure that pCC should have contacted LG5), we observed that the pCC growth cone was usually stalled and had not grown onto LG5 (Fig. 5B).

The stalled pCC phenotype probably represents a delay in growth cone extension rather than a complete block. By stage 13, the ascending pCC growth cone encounters the descending axons of dMP2 and MP1. pCC/vMP2 and MP1/dMP2 then establish a continuous longitudinal pathway (Fig. 5C). In *Ptp52F* embryos examined at a later stage than the wild-type embryo of Fig. 5C, this longitudinal pathway is still thin in ~50% of hemisegments, and the connection between pCC and the pathway appears to be missing in some hemisegments (Fig. 5D). This suggests that pCC growth cones might have retracted or taken an alternate pathway after failing to contact MP1 at the appropriate stage. By stage 15, however, the medial 1D4-positive bundle, which contains the pCC axon (Hidalgo and Brand, 1997), has a relatively normal appearance (Fig. 4B,C).

SNa pathways are altered in *Ptp52F* and double mutants

Ptp52F mutants display a variety of SNa guidance defects. The most common defect, as in *Ptp52F* RNAi embryos, is a failure to bifurcate (Fig. 6C). In other hemisegments, the SNa has extra branches (Fig. 6B), or stalls near the bifurcation point (Fig. 6D). The penetrances of such SNa phenotypes in $Ptp52F^{18.3}$

homozygotes or $Ptp52F^{18.3}/Df(2R)JP4$ transheterozygotes are 37% and 41%, respectively. The two other *Ptp52F* alleles and the transheterozygous combinations of the three *Ptp52F* alleles with *Df(2R)JP8* have a lower penetrance of SNa defects (22-28%; Table 1).

Single mutants that lack any of the other four neural RPTPs do not display SNa phenotypes. However, combinations of *Rptp* mutations do affect the SNa (Sun et al., 2001). To evaluate how removal of other RPTPs might affect *Ptp52F* SNa phenotypes, we made double mutants lacking both DPTP52F and each of the other RPTPs. We found that the absence of DPTP10D, DPTP69D or DLAR increases the penetrance of the $Ptp52F^{18.3}$ defects, particularly those in which the SNa stalls near the bifurcation point. No new phenotypes are observed in double mutants, however. Removal of DPTP99A does not affect the overall penetrance of SNa phenotypes, but does decrease the frequency of ectopic branches (Table 1).

Ptp10D Ptp52F and *Ptp52F Ptp69D* embryos display synergistic ISNb phenotypes

The ISNb motor nerve innervates the VLMs and contains the axons of the identified RP1, RP3, RP4 and RP5 motoneurons. RP growth cones leave the common ISN pathway at the exit junction, enter the VLM field, and then navigate among the muscle fibers. Synapses begin to form at stereotyped positions by late stage 16 (Fig. 7A). *Ptp52F* mutations produce any detectable ISNb phenotypes only at low frequencies (<13%; Table 2).

Fig. 4. CNS phenotypes in *Ptp52F* and double mutants. Dissected late stage 16 embryos stained with mAb 1D4. (A) wild-type. (B) *Ptp52F[18.3]*. (C) *Ptp52F[18.3]/Df(2R)JP4*. The bundles are wavy and disorganized in B,C, and the outer bundle is sometimes missing (bracket). (B,C,E) Abnormal fasciculation of the middle and outer bundles (arrowheads). (D) *Dlar[5.5]Ptp52F[18.3]*. Bundle morphology in this double mutant reverts to wild type (compare with A-C). (E) *Ptp10D[1],Ptp52F[18.3]*. (F) *Ptp52F[18.3], Ptp69D[1]/Df(3L)8ex25*. 1D4-positive bundles in these two double mutants are more disorganized than in B,C, and the middle bundle is strongly affected (asterisks). Arrow, complete connective break.
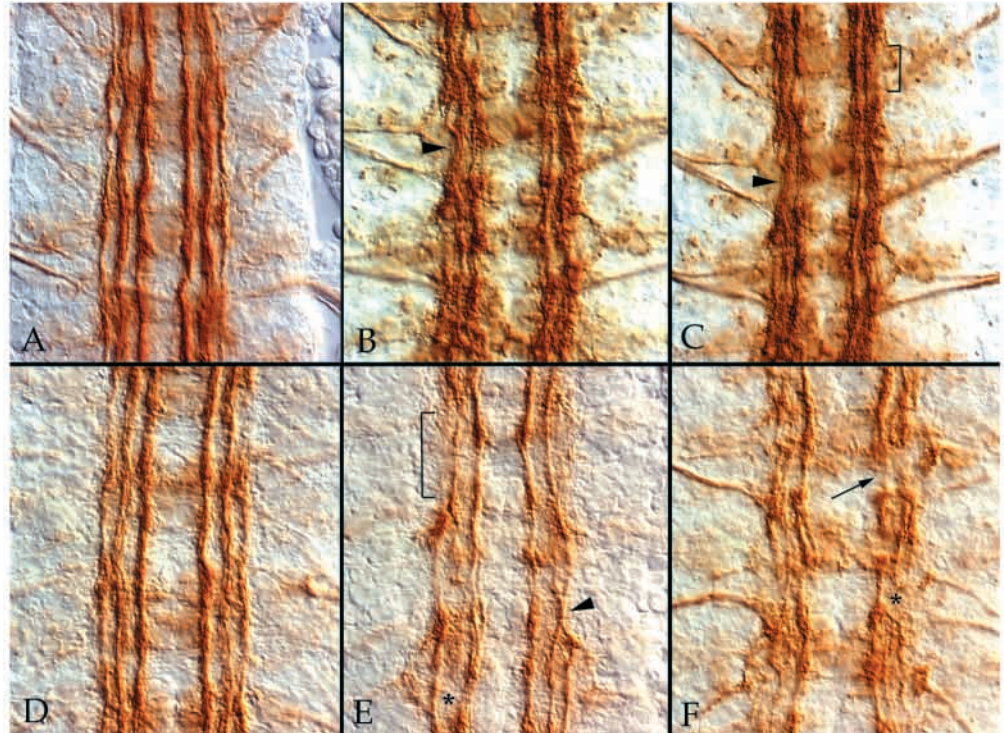
Ptp10D mutations produce no ISNb phenotypes (Sun et al., 2001). Removal of both DPTP10D and DPTP52F, however, generates a strong phenotype in which the ISNb stalls within the VLMs, often at the proximal edge of muscle 13 (Fig. 7B). This stall phenotype is observed in *Ptp52F* single mutants, but its frequency can be dramatically increased in double mutants (1%→30% for addition of a *Ptp10D* mutation to the hypomorphic mutation *Ptp52F[8.10.3]*; Table 2). Removal of DPTP69D also greatly enhances the *Ptp52F* stall phenotype (1%→20% for *Ptp52F[8.10.3]*; Table 2).

Dlar Ptp52F double mutants have parallel bypass phenotypes identical to those of *Dlar* single mutants (Krueger

et al., 1996). *Ptp99A* mutations cause no ISNb phenotypes on their own or in combination with *Ptp52F* (Table 2).

DPTP52F regulates ISN outgrowth

The ISN passes its first (FB) and second (SB) lateral branchpoints before reaching the position of its terminal arbor at the proximal edge of muscle 1 (Fig. 7C). In *Ptp52F* mutants, most ISNs are normal (Fig. 7C), but 5-17% terminate at SB (Table 3). *Dlar* mutations produce SB phenotypes with a similar penetrance (19% for null alleles) (Desai et al., 1997). When *Dlar* and *Ptp52F* mutations are combined, the frequency of the SB termination phenotype is similar to those of the single

Fig. 5. The pCC growth cone stalls in *Ptp52F* mutants. Dissected embryos stained with mAb 1D4. (A) wild-type, late stage 12. aCC growth cones (a) have just begun to turn outwards. The pCC growth cone has already grown onto the 1D4-positive LG5 cell (bracket) in the hemisegments on the right (indicated by parallel lines flanking the pCC axon connection to LG5). (B) *Ptp52F[18.3]*, early stage 13. The aCC growth cone (a) has already turned posteriorly and then begun to extend away from the CNS, but the pCC growth cones (p) have still not reached LG5. (C) Wild-type, early stage 13. The aCC growth cone (a) is at the same position as the one indicated in B. A continuous longitudinal pathway has formed. pCC axons are indicated by flanking parallel lines. (D) *Ptp52F[18.3]*, late stage 13. The aCC axons (a) have already extended beyond the edges of the panel, but there are still gaps in the longitudinal pathways on the left side (arrows) just anterior to the pCC cell bodies.
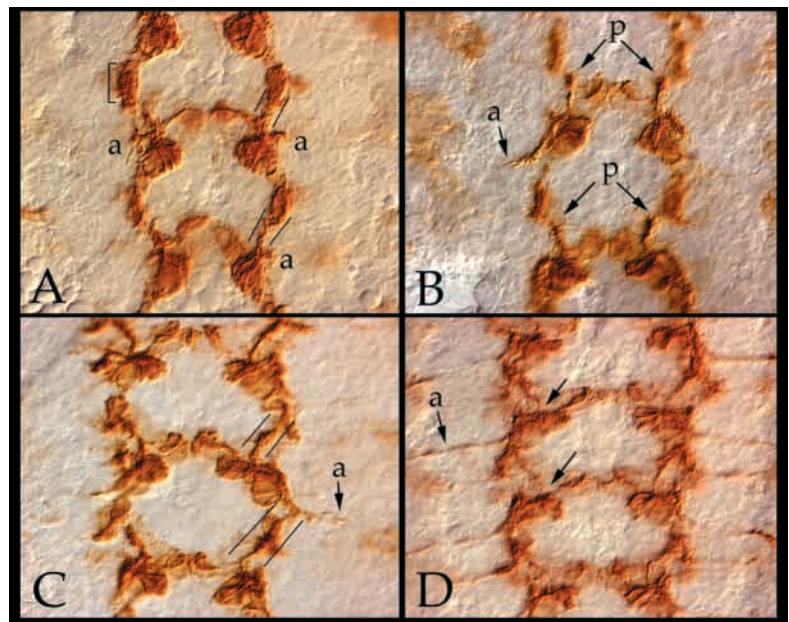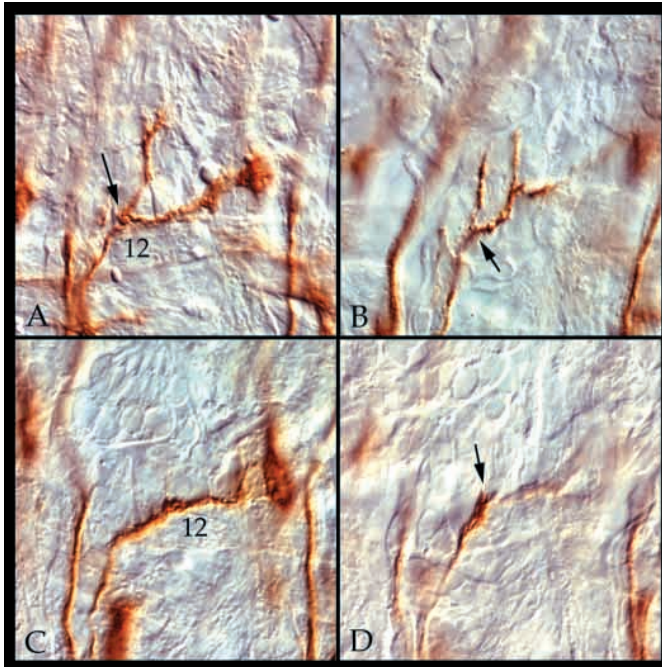
Fig. 6. SNa phenotypes in *Ptp52F* mutants. Dissected late stage 16 embryos stained with mAb 1D4. (A) Wild type. The SNa bifurcation (arrow) and muscle 12 are indicated. (B-D) *Ptp52F^18.3^*. There is an extra branch in B (arrow). The anterior branch is missing in C. Most SNa axons appear to stall near the bifurcation point in D (arrow).

mutants. *Ptp99A* mutations have no effects on ISN on their own, and also cause no enhancement of the *Ptp52F* phenotype (Table 3).

   Ptp10D and *Ptp69D* single and double mutants have no ISN phenotypes (Fig. 7D) (Sun et al., 2001). However, removal of either of these RPTPs from a *Ptp52F* mutant background enhances the penetrances of the *Ptp52F* ISN phenotypes. *Ptp10D Ptp52F* double mutants have a reduced terminal arbor (T) phenotype (35%; Fig. 7E) that is less frequently observed in *Ptp52F* single mutants (<10%). Removal of DPTP69D does not affect the T phenotype, but produces an increase in the SB phenotype (5%→40% for *Ptp52F^8.10.3^*; Table 3; Fig. 7F). In summary, our results indicate that DPTP52F, DPTP10D and DPTP69D have partially redundant functions in regulation of ISN outgrowth. It is interesting that *Ptp52F* mutations do not produce synergistic phenotypes when combined with *Dlar* mutations, which are the only other *Rptp* mutations that generate strong ISN phenotypes on their own. Perhaps there are two separate 'functions' needed for normal ISN outgrowth, one of which involves DLAR and the other DPTP52F.

Removal of DLAR suppresses the *Ptp52F* CNS phenotype

DPTP52F is the only RPTP whose removal produces clear phenotypes in the 1D4-positive longitudinal bundles of the CNS. The 1D4 pathways are usually indistinguishable from wild type in single mutants lacking each of the other four RPTPs. Removal of DPTP10D or DPTP69D from a *Ptp52F* background strengthens the *Ptp52F* CNS phenotype. The longitudinal 1D4-positive bundles become more irregular, and frequent breaks and discontinuities in the middle bundle are
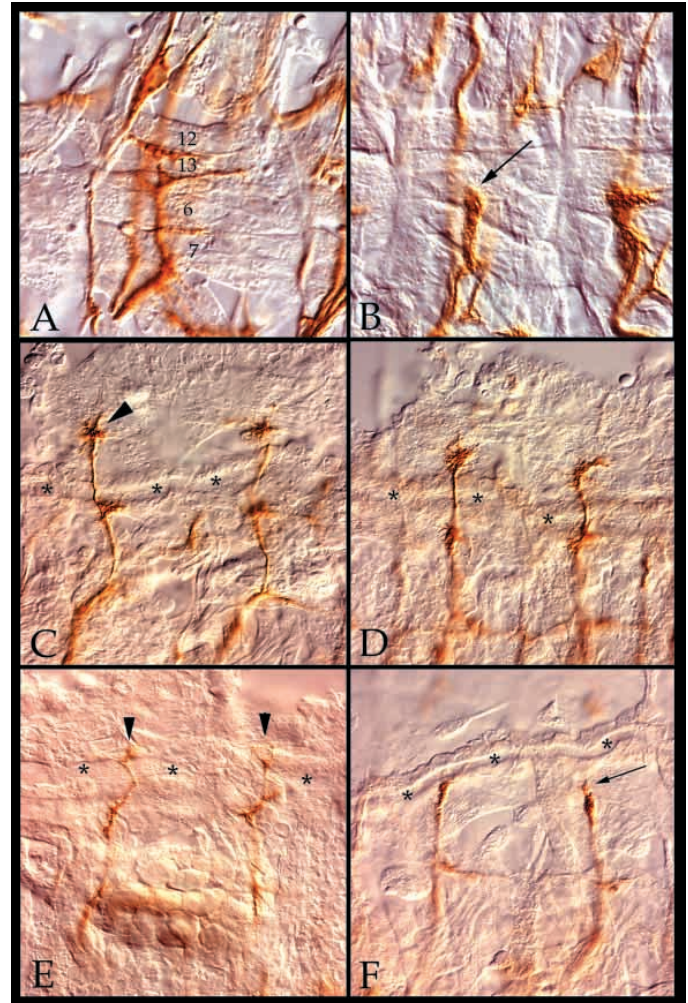

Fig. 7. ISNb and ISN phenotypes in *Ptp52F* and double mutants. Dissected late stage 16 embryos stained with mAb 1D4. (A) *Ptp52F^18.3^*. The ISNb has a normal appearance. Muscles are labeled. (B) *Ptp10D^1^, Ptp52F^8.10.3^*. The left ISNb has stalled at the proximal edge of muscle 13 (arrow) without making a synaptic branch. The right ISNb is also truncated. The distal portion of the ISN is shown in C-F. Terminal arbors are indicated by arrowheads in C,E; the large tracheal branch just distal to the second branchpoint is indicated by asterisks in C-F. (C) *Ptp52F^8.10.3^*.
(D) *Ptp69D^1^/Df(3L)8ex25*. The ISN has a normal appearance in these single mutants. (E) *Ptp10D^1^, Ptp52F^8.10.3^*. Terminal arbors are reduced in this double mutant. (F) *Ptp52F^8.10.3^, Ptp69D^1^/Df(3L)8ex25*. ISNs stall at the second branchpoint position (arrow), proximal to the tracheal branch.

observed (Fig. 4E,F). We do not, however, observe a new synergistic phenotype like that produced by removal of DPTP10D and DPTP69D together (Sun et al., 2000). Removal of DPTP99A does not affect the *Ptp52F* CNS phenotype (data not shown).

   In contrast to these results, we find that when a *Dlar* mutation is introduced into a *Ptp52F* mutant background, the morphology of the 1D4-positive bundles reverts to wild type (Fig. 4D). In a few segments of *Dlar Ptp52F* double mutants, breaks in the outer 1D4-positive bundle are still seen, but defasciculation and irregularities in the inner two bundles are not observed. The suppression is specific to the CNS

phenotypes detected at late stage 16, because the introduction of *Dlar* mutations into a *Ptp52F* mutant background does not correct the failure of the pCC growth cone to extend at the appropriate time.

DISCUSSION

We describe a new *Drosophila* RPTP, DPTP52F. This is the sixth RPTP to be identified in the fruit fly, and our analysis indicates that there are unlikely to be any other RPTPs encoded in the genome. DPTP52F is selectively expressed in CNS neurons in late embryos. We isolated mutations in the *Ptp52F* gene, and showed that *Ptp52F* mutant embryos have specific motor axon and CNS axon guidance defects. Previous studies by our group and by others have shown that mutations affecting four other RPTPs also produce axon guidance and synaptogenesis phenotypes. In summary, this work suggests that the major functions of at least five of the six *Drosophila* RPTPs are to facilitate the correct wiring of the nervous system.

RPTPs in flies, worms and humans

The existence of complete genome sequences for humans, *Drosophila* and the nematode *C. elegans* allows the determination of how many members of each gene family are required for development and function of these metazoans. We find that *Drosophila* has 14 genes encoding tyrosine-specific phosphatases: six *Rptp* genes and eight genes encoding potentially active PTPs without transmembrane domains (cytoplasmic PTPs). The two new cytoplasmic PTPs we identified are now called PEZ/CG9493 (DPTP26C) and CG7180 (DPTP36E). The completed genome sequence allowed identification of three additional PTP genes at 8F (CG3101), 61C (CG1228) and 86F (CG14714); none of these is likely to encode RPTPs (Table 4).

These conclusions differ from those in a review of kinase and phosphatase sequences in the fly genome (Morrison et al., 2000), in which CG7180 (DPTP36E) and CG4355 were classified as RPTPs. We isolated and sequenced DPTP36E cDNA clones, and these do not encode an extracellular region. CG4355 is closely related to phogrin, a transmembrane rat phosphatase-related protein expressed on secretory granules, but the *Drosophila* protein lacks the essential active-site cysteine and has no homology to the extracellular-like (lumenal) domain of phogrin.

C. elegans has many more RPTPs (15) and cytoplasmic PTPs (>57) than does the fly (Table 4) (Hutter et al., 2000; Plowman et al., 1999). To determine how many PTPs are encoded in the human genome, we examined the Celera human genome sequence database (Venter et al., 2001). Surprisingly, our analysis showed that all of the genes that are likely to encode functional human PTPs have already been identified by PCR techniques or by ESTs. The human genome appears to encode 17 active RPTPs and 16 cytoplasmic PTPs. We also found nine PTP pseudogenes that had not been previously identified.

Two human PTP-like genes (IA-2 and phogrin) encode orthologs of CG4355 in *Drosophila* and *ida-1* in *C. elegans* (Zahn et al., 2001). All of these proteins contain sequence changes at crucial positions, indicating that they do not

Table 4. PTPs in the *Drosophila* genome

(A) PTP superfamily genes in fly, worm and human

Group	Fly	Fly fragments	Worm*	Worm fragments*	Human
cPTP	8	2	57	4	17[‡]
RPTP	6	0	26? (15)	14?	16
DSP	13	4	65	0	n.d.
LMW	2	0	n.d.	n.d.	n.d.

(B) Complete tyrosine-specific phosphatases

GG	Name	Type	Domains	Worm ortholog
6899	DPTP4E	RPTP	FN3	F44G4.8 (1e-100)
1817	DPTP10D	RPTP	FN3	F44G4.8 (4.4e-104)
10443	DLAR	RPTP	FN3, Ig	C09D8.1 (0.0)
18243	DPTP52F	RPTP	FN3	–
10975	DPTP69D	RPTP	FN3, Ig	CLR-1 (1.1e-101) *or* C09D8.1 (2e-103)
2005	DPTP99A	RPTP	FN3	K04D7.4 (6.3e-82)
9181	DPTP61F	cPTP		–
3954	CSW	cPTP	SH2	PTP-2 (1.4e-70)
1228	PTPMEG	cPTP	PDZ, ezrin	PTP-1 (6.1e-156)
9493	PEZ	cPTP	Ezrin	C48D5.2A (4e-36)
9856	PTP-ER	cPTP		–
3101		cPTP		–
14714		cPTP		–
7180		cPTP		T13H5.1 (1.3e-108)

*Data from Plowman et al. (Plowman et al., 1999). Hutter et al. (Hutter et al., 2000), however, find only 15 worm RPTPs, and we concur with this number.

‡There are also two inactive PTP-like proteins, and at least nine pseudogenes.

cPTP, cytoplasmic PTP; DSP, dual-specificity phosphatase; FN3, fibronectin type III repeat; Ig, immunoglobulin-like domain; LMW, low molecular weight phosphatase; n.d., not determined; RPTP, receptor-linked PTP; –, no clear ortholog.

function as active phosphatases (Cai et al., 2001; Magistrelli et al., 1996).

Three of the six *Drosophila* RPTPs have human and *C. elegans* counterparts, as follows:

(1) The DPTP10D/DPTP4E subfamily (Type III) is characterized by a large number of FN3 repeats (≥8) and a single PTP domain. It has a single member in *C. elegans* (F44G4.8), two members in *Drosophila* (DPTP10D and DPTP4E), and five members in humans (HPTPβ, HPTPη, GLEPP-1, Sap-1 and PTP-RQ). PTP-RQ is only defined in humans by a 134 amino acid fragment, but our analysis indicates that the complete protein is >2000 amino acids and is the ortholog of rat rPTP-GMC1.

(2) The LAR subfamily (Type IIa) has three Ig domains and eight or nine FN3 repeats, and two PTP domains. It has a single member in *C. elegans* (C09D8.1) and *Drosophila* (DLAR) and three members in humans (LAR, PTPδ, and PTPσ).

Two other fly RPTPs have counterparts in *C. elegans* but no obvious human orthologs:

(1) DPTP69D has two Ig domains and three FN3 repeats, and is probably orthologous to *C. elegans* CLR-1.

(2) DPTP99A corresponds to worm K04D7.4. It has three FN3 repeats and two PTP domains, but the second domain lacks the essential cysteine residue. DPTP69D and DPTP99A have been classified as Type IIa (LAR-like) and Type III

(DPTP10D-like), respectively, but this may be incorrect, as their domain organizations differ from the other members of these subfamilies.

DPTP52F does not have clear nematode or human orthologs. It is equally related to a number of different PTPs. DPTP52F might be classified as a member of the DPTP10D/DPTP4E (Type III) subfamily, however, as it has an XC domain with FN3 repeats and only one cytoplasmic PTP domain.

The 11 *C. elegans* RPTPs that are not orthologous to *Drosophila* or human RPTPs all have a nematode-specific extracellular domain denoted as FE (Hutter et al., 2000). This domain has no close relatives in *Drosophila* or other sequenced species.

The human genome encodes nine RPTPs in four subfamilies not found in worms or flies: (1) MAM domain RPTPs (Type IIb), some of which can function as homophilic adhesion molecules (PTPμ, PTPκ, PTPρ and PTPο); (2) Carbonic anhydrase domain-containing (Type V) RPTPs (PTPζ and PTPγ); (3) Type IV RPTPs, which have short glycosylated extracellular domains (PTPα and PTPε); and (4) CD45 (Type I). (Most human RPTPs have several names, and one name was arbitrarily selected here; see Materials and Methods for listings of all names).

Regulation of axon guidance by DPTP52F

To evaluate the functions of DPTP52F during development, we first used RNAi to inhibit its expression. *Ptp52F* RNAi embryos have distinctive motor axon and CNS phenotypes (Fig. 3). We used these phenotypes as a tool for analysis of a set of lethal mutations within the interval containing the *Ptp52F* gene. Mutations in one complementation group produced phenotypes identical to those observed with RNAi. We sequenced the *Ptp52F* gene from three mutant lines and found nonconservative missense substitution mutations (Fig. 1). Embryos from all three mutant lines fail to stain with anti-DPTP52F mAb, suggesting that the mutant proteins do not fold correctly or are unstable (Fig. 2).

We characterized motor axon phenotypes produced by these mutations. In *Ptp52F* mutants, the SNa motor nerve fails to bifurcate in a normal manner in about 40% of hemisegments (Table 1). SNa normally splits into anterior and posterior branches at a choice point just distal to muscle 12. Mutant SNa nerves lack either the anterior or posterior branches with approximately equal frequency. SNa nerves can also have ectopic branches or stall near the normal bifurcation point (Fig. 6).

To further examine the roles of DPTP52F in regulating motor axon guidance, we made double mutants lacking DPTP52F together with each of the other four neural RPTPs. Our earlier work has defined three modes of genetic interaction among *Rptp* genes: partial redundancy (a guidance decision can be facilitated by any one of a set of RPTPs), collaboration (expression of two specific RPTPs is required to allow a decision to take place) and competition (loss-of-function mutations in one *Rptp* gene suppress a phenotype produced by mutations in the other gene). Some of these genetic interactions could be explained by formation of RPTP heteromultimers (Sun et al., 2001).

Ptp52F exhibits both partial redundancy and competition in its interactions with the other Rptp genes. It has strong interactions with *Ptp10D*, *Dlar* and *Ptp69D*, but not with *Ptp99A*. Interactions with *Ptp10D* and *Ptp69D* are synergistic: both the CNS and motor axon phenotypes are worsened in double mutants. In some cases, there is a dramatic difference between double mutants and either single mutant. For example, the ISNb stall phenotype is almost never observed in either *Ptp52F* (hypomorph) or *Ptp10D* mutants (1% of hemisegments), while 30% of hemisegments have this phenotype in double mutants (Table 2). These kinds of interactions suggest that some process needed for ISNb extension through the VLM field can be mediated by either DPTP10D or DPTP52F, and this process only fails when both are missing.

Ptp52F embryos have longitudinal tract phenotypes in which the 1D4-positive bundles are irregular and the outer bundle is often missing. These phenotypes are absent in *Dlar Ptp52F* double mutants, suggesting that DLAR and DPTP52F interact in a competitive manner to regulate longitudinal tract axon guidance/outgrowth decisions (Fig. 4). *Dlar* does not suppress the *Ptp52F* SNa or ISN phenotypes, however, so these two RPTPs do not always interact competitively.

DLAR also participates in another competitive interaction: the *Dlar* ISNb parallel bypass phenotype is absent in *Dlar Ptp99A* double mutants (Desai et al., 1997). Here, however, it is a *Dlar* phenotype that is suppressed by removal of another RPTP, rather than the reverse. *Ptp52F* mutations do not affect *Dlar* parallel bypass phenotypes. Determination of the mechanisms that underlie these genetic interactions will require biochemical analysis of DPTP5F and of the signaling pathways in which it participates.

REFERENCES

Cai, T., Krause, M. W., Odenwald, W. F., Toyama, R. and Notkins, A. L. (2001). The IA-2 gene family: homologs in Caenorhabditis elegans, Drosophila and zebrafish. *Diabetologia* **44**, 81-88.

Desai, C. J., Popova, E. and Zinn, K. (1994). A Drosophila receptor tyrosine phosphatase expressed in the embryonic cns and larval optic lobes is a member of the set of proteins bearing the HRP carbohydrate epitope. *J. Neurosci.* **14**, 7272-7283.

Desai, C. J., Gindhart Jr., J. G., Goldstein, L. S. B. and Zinn, K. (1996). Receptor tyrosine phosphatases are required for motor axon guidance in the Drosophila embryo. *Cell* **84**, 599-609.

Desai, C. J., Krueger, N. X., Saito, H. and Zinn, K. (1997). Competition and cooperation among receptor tyrosine phosphatases control motoneuron growth cone guidance in drosophila. *Development* **124**, 1941-1952.

Fashena, S. J. and Zinn, K. (1997). The transmembrane glycoprotein gp150 is a substrate for the receptor tyrosine phosphatase DPTP10D in *Drosophila* cells. *Mol. Cell. Biol.* **17**, 6859-6867.

Fauman, E. B. and Saper, M. A. (1996). Structure and function of the protein tyrosine phosphatases. *Trends Biochem. Sci.* **21**, 413-417.

Garrity, P. A., Lee, C. H., Salecker, I., Robertson, H. C., Desai, C. J., Zinn,

K. and Zipursky, S. L. (1999). Retinal axon target selection in *Drosophila* is regulated by a receptor protein tyrosine phosphatase. *Neuron* 22, 707-717.

Hamilton, B. A., Ho, A. and Zinn, K. (1995). Targeted mutagenesis and genetic analysis of a *Drosophila* receptor-linked protein tyrosine phosphatase gene. *Roux's Arch. Dev. Biol.* 204, 187-192.

Hariharan, I., Chuang, P.-T. and Rubin, G. M. (1991). Cloning and characterization of a receptor-class phosphotyrosine phosphatase gene expressed on central nervous system axons in *Drosophila melanogaster*. *Proc. Natl. Acad. Sci. USA* 88, 11266-11270.

Hidalgo, A. and Brand, A. H. (1997). Targeted neuronal ablation-the role of pioneer neurons in guidance and fasciculation in the CNS of *Drosophila*. *Development* 124, 3253-3262.

Hutter, H., Vogel, B. E., Plenefisch, J. D., Norris, C. R., Proenca, R. B., Spieth, J., Guo, C. B., Mastwal, S., Zhu, X. P., Scheel, J. et al. (2000). Cell biology: Conservation and novelty in the evolution of cell adhesion and extracellular matrix genes. *Science* 287, 989-994.

Karim, F. D. and Rubin, G. M. (1999). PTP-ER, a novel tyrosine phosphatase, functions downstream of Ras1 to downregulate MAP kinase during Drosophila eye development. *Mol. Cell* 3, 741-750.

Kennerdell, J. R. and Carthew, R. W. (1998). Use of dsRNA-mediated genetic interference to demonstrate that frizzled and frizzled 2 act in the wingless pathway. *Cell* 95, 1017-1026.

Keshishian, H., Broadie, K., Chiba, A. and Bate, M. (1996). The *Drosophila* neuromuscular junction: A model for studying development and function. *Annu. Rev. Neurosci.* 19, 545-575.

Krueger, N. X., Van Vactor, D., Wan, H. I., Gelbart, W. M., Goodman, C. S. and Saito, H. (1996). The transmembrane tyrosine phosphatase DLAR controls motor axon guidance in Drosophila. *Cell* 84, 611-622.

Magistrelli, G., Toma, S. and Isacchi, A. (1996). Substitution of two variant residues in the protein tyrosine phosphatase-like PTP35/IA-2 sequence reconstitutes catalytic activity. *Biochem. Biophys. Res. Commun.* 227, 581-588.

McLaughlin, S. and Dixon, J. E. (1993). Alternative splicing gives rise to a nuclear protein tyrosine phosphatase in *Drosophila*. *J. Biol. Chem.* 268, 6839-6842.

Misquitta, L. and Paterson, B. M. (1999). Targeted disruption of gene function in Drosophila by RNA interference (RNA-i): A role for nautilus in embryonic somatic muscle formation *Proc. Natl. Acad. Sci. USA* 96, 1451-1456.

Morrison, D. K., Murakami, M. S. and Cleghon, V. (2000). Protein kinases and phosphatases in the Drosophila genome. *J. Cell Biol.* 150, F57-F62.

Newsome, T. P., Asling, B. and Dickson, B. J. (2000). Analysis of Drosophila photoreceptor axon guidance in eye-specific mosaics. *Development* 127, 851-860.

Oon, S. H., Hong, A., Yang, X. H. and Chia, W. (1993). Alternative splicing in a novel tyrosine phosphatase gene (DPTP4E) of Drosophila-melanogaster generates 2 large receptor-like proteins which differ in their carboxyl termini. *J. Biol. Chem.* 268, 23964-23971.

Patel, N. H. (1994). Imaging neuronal subsets and other cell types in whole-mount Drosophila embryos and larvae using antibody probes. In Drosophila melanogaster*: Practical Uses in Cell and Molecular Biology*. Vol. 44 (ed. E. Fyrberg and L. S. B. Goldstein), pp. 446-488. San Diego, CA: Academic Press.

Perkins, L. A., Larsen, I. and Perrimon, N. (1992). *corkscrew* encodes a putative protein tyrosine phosphatase that functions to transduce the terminal signal from the receptor tyrosine kinase torso. *Cell* 70, 225-236.

Plowman, G. D., Sudarsanam, S., Bingham, J., Whyte, D. and Hunter, T. (1999). The protein kinases of Caenorhabditis elegans: A model for signal transduction in multicellular organisms. *Proc. Natl. Acad. Sci. USA* 96, 13603-13610.

Schmid, A., Schindelholz, B. and Zinn, K. (2001). Combinatorial RNAi: a method for evaluating the functions of gene families in *Drosophila*. *Trends Neurosci*. (in press).

Seeger, M., Tear, G., Ferres-Marco, D. and Goodman, C. S. (1993). Mutations affecting growth cone guidance in Drosophila: genes necessary for guidance toward or away from the midline. *Neuron* 10, 409-426.

Streuli, M., Krueger, N. X., Tsai, A. Y. M. and Saito, H. (1989). A family of receptor-linked protein tyrosine phosphatases in humans and *Drosophila*. *Proc. Natl. Acad. Sci. USA* 86, 8698-8702.

Sun, Q., Bahri, S., Schmid, A., Chia, W. and Zinn, K. (2000). Receptor tyrosine phosphatases regulate axon guidance across the midline of the Drosophila embryo. *Development* 127, 801-812.

Sun, Q., Schindelholz, B., Knirr, M., Schmid, A. and Zinn, K. (2001). Complex genetic interactions among four receptor tyrosine phosphatases regulate axon guidance in Drosophila. *Mol. Cell. Neurosci.* 17, 274-291.

Tian, S.-S., Tsoulfas, P. and Zinn, K. (1991). Three receptor-linked protein-tyrosine phosphatases are selectively expressed on central nervous system axons in the *Drosophila* embryo. *Cell* 67, 675-685.

Van Vactor, D., Sink, H., Fambrough, D., Tsoo, R. and Goodman, C. S. (1993). Genes that control neuromuscular specificity in Drosophila. *Cell* 73, 1137-1153.

Venter, J. C., Adams, M. D., Myers, E. W., Li, P. W., Mural, R. J., Sutton, G. G., Smith, H. O., Yandell, M., Evans, C. A., Holt, R. A. et al. (2001). The sequence of the human genome. *Science* 291, 1304-1353.

Walchli, S., Colinge, J. and van Huijsduijnen, R. H. (2000). MetaBlasts: tracing protein tyrosine phosphatase gene family roots from Man to Drosophila melanogaster and Caenorhabditis elegans genomes. *Gene* 253, 137-143.

Wills, Z., Bateman, J., Korey, C. A., Comer, A. and Van Vactor, D. (1999). The tyrosine kinase Abl and its substrate Enabled collaborate with the receptor phosphatase Dlar to control motor axon guidance. *Neuron* 22, 301-312.

Yang, X., Seow, K. T., Bahri, S. M., Oon, S. H. and Chia, W. (1991). Two Drosophila receptor-like tyrosine phosphatase genes are expressed in a subset of developing axons and pioneer neurons in the embryonic CNS. *Cell* 67, 661-673.

Zahn, T. R., Macmorris, M. A., Dong, W. J., Day, R. and Hutton, J. C. (2001). IDA-1, a Caenorhabditis elegans homolog of the diabetic autoantigens IA-2 and phogrin, is expressed in peptidergic neurons in the worm. *J. Comp. Neurol.* 429, 127-143.

Zinn, K., McAllister, L. and Goodman, C. S. (1988). Sequence analysis and neuronal expression of fasciclin I in grasshopper and Drosophila. *Cell* 53, 577-587.

Zinn, K. and Sun, Q. (1999). Slit branches out: a secreted protein mediates both attractive and repulsive axon guidance. *Cell* 97, 1-4.